

# Fast Transient Thermal Analysis of Gold Nanoparticles in Tissue-Like Medium

Changhong Liu, Ben Q. Li, and Chunting Chris Mi\*, *Senior Member, IEEE*

**Abstract**—Gold-nanoparticle-based hyperthermia has attracted considerable attention in the recent ten years in cancer treatment. In hyperthermia-based cancer treatment, in order to produce efficient thermal therapy yet without excessive heat damage to human body, besides the steady-state thermal condition, the transient thermal response is of vital importance. As part of theoretical research associated with nanoparticle-mediated hyperthermia therapy for cancer treatment, the transient heat transfer process of laser interacting with gold nanoparticle in tissue-like medium is investigated. Within the framework of dual-phase-lag (DPL) model, this paper focuses on the microscopic heat transfer performance of a gold nanoparticle in a surrounding medium. A semianalytical solution of 1-D nonhomogenous DPL equation in spherical coordinates is presented for a heat transfer process with a constant laser heat source and a short-pulsed laser heating source. Results show that the transient temperature calculated by DPL model greatly exceeds that predicted by the classical diffusion model, with either a constant source or a pulsed source. This phenomenon is mainly attributed by the phase lag of heat flux in the surrounding tissue.

**Index Terms**—Diffusion model, dual-phase-lag (DPL) model, gold nanoparticle, transient thermal response.

## NOMENCLATURE

$a$	Particle radius (in meters).
$A$	Coefficient in (9).
$b$	Coefficient in (16).
$C_{i1}$	Coefficient in (13).
$C_{i2}$	Coefficient in (13).
$C_e$	Volumetric heat capacity of electron [in joules per(cubic meter-kelvin)].
$C_l$	Volumetric heat capacity of lattice [in joules per(cubic meter-kelvin)].
$C_p$	Specific heat [in joules per (kilogram-kelvin)].
$D$	Coefficient in (9).
$E$	Coefficient in (12).
$g$	Reciprocal of penetration depth.
$J$	Intensity of laser pulse (in joules per square meter).
$k$	Thermal conductivity [in watts per(meter-kelvin)].

Manuscript received August 27, 2008; revised April 5, 2009. Current version published January 4, 2010. This work was supported by the grants from the Office of the Vice President for Research, University of Michigan. *Asterisk indicates corresponding author.*

C. Liu is with Shanghai Jiao Tong University, Shanghai 200030, China, and also with the Department of Electrical and Computer Engineering, University of Michigan-Dearborn, Dearborn, MI 48128 USA (e-mail: lchsh@umd.umich.edu).

B. Q. Li is with the Department of Mechanical Engineering, University of Michigan-Dearborn, Dearborn, MI 48128 USA (e-mail: benqli@umich.edu).

\*C. C. Mi is with the Department of Electrical and Computer Engineering, University of Michigan-Dearborn, Dearborn, MI 48128 USA (e-mail: chrismi@umich.edu).

Color versions of one or more of the figures in this paper are available online at <http://ieeexplore.ieee.org>.

Digital Object Identifier 10.1109/TNB.2009.2028885

$p$	Laplacian parameter.
$q$	Heat flux (in watts per square meter).
$r$	Radial coordinate (in meters).
$Q$	Volumetric heating source (in watts per cubic meter).
$R$	Reflectivity.
$S$	Volumetric heating source (in watts per cubic meter).
$t$	Time (in seconds).
$T$	Temperature (in kelvins).
$T_0$	The initial temperature (in kelvins).
$\bar{U}$	Dimensionless variable in Laplacian transform domain.
$W$	Dimensionless volumetric heating source.

## Greek symbols

$\alpha$	Thermal diffusivity (in square meters per second).
$\beta$	Dimensionless time.
$\gamma$	Coefficient.
$\delta$	Dimensionless radial coordinate.
$\eta$	Dimensionless heat flux.
$\lambda$	Dimensionless particle radius.
$\tau_q$	Phase lag of heat flux (in seconds).
$\tau_T$	Phase lag of temperature gradient (in seconds).
$\Theta$	Dimensionless temperature.
$\bar{\Theta}$	Laplace transform of dimensionless temperature.

## Subscript

$i$	Lyer number.
1	Particle or inner layer.
2	Tissue or outer layer.
$s$	Steady state.
$r$	Reference variable.
$p$	Laplace transform domain.
$T$	Temperature gradient.
$q$	Heat flux.

## I. INTRODUCTION

**G**OLD nanoparticles have received considerable attentions in cancer treatment in the recent ten years. This is due to the unique optical properties exhibited by spherical particles at nanoscale. There exists significant local electric field enhancement near metal-dielectric interface due to the strong localized surface plasmon resonance (LSPR) and the high tunability of LSPR frequency [1], [2]. When exposed to a laser beam with appropriate wavelengths, the nanoparticles preembedded in a tumor absorb energy, and then heat up, but the healthy tissues along the laser path do not. With temperature increasing, cancerous cells gradually lose activity. The treatment at a temperature between 40 °C and 44 °C is believed cytotoxic for cells in an environment with hypoxia and low pH, conditions that are found to be largely associated with tumor tissue, but not in normal tissues [3], [4]. This makes the nanoparticle-based

thermotherapy superior to other traditional treatments for non-invasive and targeted therapy of cancer patients. Although this promising idea has been principally confirmed in experiments on small animals [5], [6], the corresponding theoretical research, to our best knowledge, has not been conducted systematically. Consequently, there is a lack of fundamental understanding of the interaction between laser and tissue, and laser and nanoparticles. Developing such understanding requires the analysis of heat transfer at a local microscale. From the clinic application point of view, quantitative relationships need to be established for a thermal dose based on the intensity, style, and irradiating time of laser. In order to produce efficient thermotherapy yet without excessive heat damage to human body, besides the steady-state thermal condition, the transient thermal response is of vital importance.

For most engineering applications, the heat conduction can be described by classical diffusion equation. However, there exist regimes of space and time where such macroscopic equations are no longer applicable. This has been proved in many literatures [7]–[10]. Within the macroscopic framework, temperature field is assumed not only to be continuum, but also holding thermoequilibrium at every location. However, when length scale is comparable to or smaller than the mean free path of the material (at room temperature, the mean free path of gold is around 38 nm), the macroscopic model is of question. Since there are no sufficient energy carriers in the interested direction, the temperature field is discontinuous. Once the concept of temperature gradient fails, the classical Fourier's law is also questionable, so is the associated diffusion equation. A similar situation exists in the response time for temperature. Macroscopic heat equation assumes that temperature gradient follows simultaneously with heat flux vector. In fact, any physical process needs a finite time to take place, so does the heat energy transfer in media. As a result, once the response time of primary concern is of the same order of magnitude as the mean free time, the lagging behavior caused by phonon–electron interaction in metal films or phonon scattering in dielectric media must be taken into account. For most metals, mean free time or relaxation time is in the order of picoseconds. For dielectric crystal, it is in the order of nanoseconds to picoseconds.

In nanoparticle-based hyperthermia, hundreds of thousands gold nanoshells, with shell thickness of 2–10 nm, absorb heat from either continuous wave (CW) laser or pulsed wave (PW) laser source. It is generally believed that pulsed laser produces more locally concentrated energy and more penetration depth in media [11]. Hence, short pulsed laser with very short duration is widely used in medical applications. Due to the fact that short pulsed laser interacting with nanoparticles determines the microscopic nature of heat transfer from both microstructure and microtime scale point of view, microscopic heat conduction model should be used instead of macroscopic model. So far, to the best of our knowledge, few publications studied the heat transfer mechanism of nanoparticle-based hyperthermia from the microscopic perspective.

The purpose of this paper is to investigate the fast transient thermal response of both nanoparticles and tissue under constant and pulsed heat sources. This paper is considered a continuation

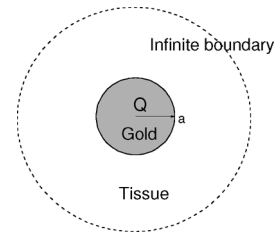


Fig. 1. Schematic diagram for laser heating.

of the electromagnetic analysis of laser–nanoparticle interaction published earlier [12], where some preliminary data on the frequency tunability of plasmonic gold nanoparticles and animal experiments that validated the concept of the heat generation through particle–laser interaction were presented. As a first step, a single solid gold sphere embedded in infinite tissue-like media is considered (see Fig. 1). The heat generation inside the particle is assumed uniformly distributed. Thus, the mathematical model reduces to a transient 1-D nonhomogenous heat conduction problem in spherical coordinate. Constant heat source and pulsed laser heat source are studied. A Laplace-transform-based solution for transient heat transfer within the framework of dual-phase-lag (DPL) model is presented. It should be noted that although the actual geometry shape and heat sources in real application may differ from a constant one, the analysis should be helpful in gaining physical insight into the behavior of the nanoparticle at spatial and temporal scales.

## II. MATHEMATICAL FORMULATION

In order to consider the effect of microstructured interaction at very short time scale, Tzou proposed the DPL model, which describes microscopic thermal phenomenon by modifying the macroscopic description of heat conduction [13]. The physical explanation and the effect has been validated by experimental results [13], [14], and the model proves to be useful in the study of transient energy transport processes in single- and multilayered materials [15]–[20].

As stated in [13], due to finite wave speed, heat flux vector and temperature gradient occur at different instants of time. Compared to Fourier's law, the constitutive equation can be written as

$$\vec{q}(\vec{r}, t + \tau_q) = -k\nabla T(\vec{r}, t + \tau_T) \quad (1)$$

where  $t$  is time instant at which conservation of energy is imposed and  $\tau_q$  is the phase lag of the heat flux vector. At time instant  $t + \tau_q$ , heat flows through the material volume and  $\tau_T$  is the phase lag of temperature gradient. At time instant  $t + \tau_T$ , temperature gradient is established across a material volume. Obviously, in the DPL model presented before, the microscopic thermal phenomenon are lumped into two delayed response time to predict the thermobehavior in microscale. Tang and Araki interpreted the physical explanation of these two parameters from the microscale sense [15]. For dielectric crystals, by comparing DPL model with the pure phonon field model [21], it can be found that  $\tau_q$  is the relaxation time for the momentum nonconserving process and  $\tau_T$  is the relaxation time for the normal

process conserving the momentum in the phonon system. For metals, by comparing with the micro-two-step model [22], it is found that  $\tau_T$  captures the time delay due to the microstructural interaction effect, namely, the finite time required for phonon–electron interaction to take place and  $\tau_q$  captures the time delay due to the fast transient effect of thermal inertia. The two parameters  $\tau_T$  and  $\tau_q$  account for the time required by both heat flux and temperature gradient to gradually respond to thermal disturbances, such as an imposed temperature difference or heating.

The first-order expansion of (1) with respect to  $t$  is

$$\vec{q}(\vec{r}, t) + \tau_q \frac{\partial \vec{q}(\vec{r}, t)}{\partial t} \approx -k \left\{ \nabla T(\vec{r}, t) + \tau_T \frac{\partial}{\partial t} [\nabla T(\vec{r}, t)] \right\}. \quad (2)$$

Taking the divergence of (2) and substituting  $\nabla \cdot \vec{q}$  to the energy equation established at a general time  $t$

$$-\nabla \cdot \vec{q}(\vec{r}, t) + Q(\vec{r}, t) = C_p \frac{\partial T(\vec{r}, t)}{\partial t}. \quad (3)$$

The  $T$  representation of the DPL model is

$$\nabla^2 T + \tau_T \frac{\partial}{\partial t} \nabla^2 T + \frac{1}{K} \left[ Q + \tau_q \frac{\partial Q}{\partial t} \right] = \frac{1}{\alpha} \frac{\partial T}{\partial t} + \frac{\tau_q}{\alpha} \frac{\partial^2 T}{\partial t^2} \quad (4)$$

subject to the following boundary conditions:

$$\begin{aligned} T_1(a, t) &= T_2(a, t) \\ q_1(a, t) &= q_2(a, t) \\ \frac{\partial T_1(0, t)}{\partial r} &= 0 \\ T_2(\infty, t) &= T_0 \end{aligned} \quad (5)$$

and initial condition

$$T(r, 0) = T_0.$$

It should be noted that when  $\tau_q = \tau_T$ , (1) reduces to Fourier's law, and DPL model in (4) becomes the classical diffusion equation. If  $\tau_T = 0$ , (4) becomes the CV wave model originated by Cattaneo and Vernotte. The DPL mode can also be developed to the hyperbolic two-step model, the parabolic two-step model, Jeffreys type heat flux model, and microscopic phonon-scattering model [13].

### III. SEMIANALYTICAL SOLUTION

#### A. Constant Heat Source

By introducing the following dimensionless variables:

$$\begin{aligned} \Theta &= \frac{T - T_r}{T_r}, \quad \beta = \frac{t}{\tau_{qr}}, \quad \delta = \frac{r}{\sqrt{\alpha_r \tau_{qr}}}, \quad \alpha_{ri} = \frac{\alpha_i}{\alpha_r}, \\ K_{ri} &= \frac{K_i}{K_r}, \quad \tau_{Tri} = \frac{\tau_{Ti}}{\tau_{qr}}, \quad \tau_{qri} = \frac{\tau_{qi}}{\tau_{qr}}, \quad \text{and} \\ W &= \frac{Q}{k_r T_r / \alpha_r \tau_{qr}}. \end{aligned}$$

Equation (4) in spherical coordinates can be written as

$$\begin{aligned} \left( \frac{\partial^2 \Theta}{\partial \delta^2} + \frac{2}{\delta} \frac{\partial \Theta}{\partial \delta} \right) + \tau_{Tri} \frac{\partial}{\partial \beta} \left( \frac{\partial^2 \Theta}{\partial \delta^2} + \frac{2}{\delta} \frac{\partial \Theta}{\partial \delta} \right) \\ + \frac{W}{K_{ri}} = \frac{1}{\alpha_{ri}} \frac{\partial \Theta}{\partial \beta} + \frac{\tau_{qri}}{\alpha_{ri}} \frac{\partial^2 \Theta}{\partial \beta^2}. \end{aligned} \quad (6)$$

Applying the Laplace transform to (6) yields

$$\left( \frac{\partial^2 \bar{\Theta}}{\partial \delta^2} + \frac{2}{\delta} \frac{\partial \bar{\Theta}}{\partial \delta} \right) - \frac{(1 + \tau_{qri} p)}{\alpha_{ri} (1 + \tau_{Tri} p)} \bar{\Theta} + \frac{1}{K_{ri} (1 + \tau_{Tri} p) p} W = 0. \quad (7)$$

Introducing  $\bar{\Theta} = \bar{U} / \delta$ , with some algebraic manipulations, (7) becomes

$$\frac{\partial^2 \bar{U}}{\partial \delta^2} - \frac{(1 + \tau_{qri} p)}{\alpha_{ri} (1 + \tau_{Tri} p)} \bar{U} + \frac{1}{K_{ri} (1 + \tau_{Tri} p) p} W \delta = 0. \quad (8)$$

We then introduce

$$A_i = \frac{(1 + \tau_{qri} p)}{\alpha_{ri} (1 + \tau_{Tri} p)}, \quad D_i = \frac{1}{K_{ri} (1 + \tau_{Tri} p) p} W$$

with  $i = 2$ ,  $D_2 = 0$ , (8) is further simplified as

$$\frac{\partial^2 \bar{U}}{\partial \delta^2} - A_i \bar{U} + D_i \delta = 0. \quad (9)$$

The aforementioned equation is a differential equation written in the nondimensionless variables in the Laplacian transform domain. It is straightforward to obtain the general solution of  $\bar{\Theta}$  to (9) in the following form:

$$\bar{\Theta}_i(\delta; p) = \frac{\bar{U}_i(\delta; p)}{\delta} = \frac{D_i}{A_i} + \frac{C_{i1} e^{\sqrt{A_i} \delta} + C_{i2} e^{-\sqrt{A_i} \delta}}{\delta}. \quad (10)$$

By introducing nondimensional heat flux variable

$$\eta = \frac{q}{k_r T_r / \sqrt{\alpha_r \tau_{qr}}}$$

boundary conditions in (5) are rewritten as follows:

$$\begin{cases} \Theta_1 = \Theta_2 & \text{as } r = a \\ \eta_1 = \eta_2 & \text{as } r = a \\ \frac{\partial \Theta_1}{\partial \delta} = 0 & \text{as } r = 0 \\ \Theta_2 = 0 & \text{as } r = \infty. \end{cases} \quad (11)$$

Applying dimensionless analysis and taking Laplace transform with respect to  $\beta$

$$\bar{\eta}(\delta; p) \approx -E_i \frac{\partial \bar{\Theta}}{\partial \delta} \quad (12)$$

where

$$E_i = \frac{K_{ri} (1 + \tau_{Tri} p)}{1 + \tau_{qri} p}.$$

Substituting (10) into (12), the following expression is obtained:

$$\bar{\eta}_i(\delta; p) \approx -\frac{K_{ri}(1 + \tau_{Tri}p)}{1 + \tau_{qri}p} \left( -\frac{C_{i1}e^{\sqrt{A_i}\delta} + C_{i2}e^{-\sqrt{A_i}\delta}}{\delta^2} + \frac{C_{i1}\sqrt{A_i}e^{\sqrt{A_i}\delta} - C_{i2}\sqrt{A_i}e^{-\sqrt{A_i}\delta}}{\delta} \right). \quad (13)$$

The four coefficients in (10) can thus be determined from (11) and the solution of  $\bar{\Theta}$  in the Laplace transform domain takes the following form, (14), as shown at the bottom of this page, where  $\lambda_1 = a/\sqrt{\alpha_1\tau_{q1}}$ .

The Laplacian inversion of (14) is computed using the Riemann sum approximation given by [13]

$$\Theta(\delta, \beta) = \frac{e^{\gamma\beta}}{\beta} \left[ \frac{1}{2}\bar{\Theta}(\delta, \gamma) + \text{Re} \sum_{n=1}^{\infty} \bar{\Theta}\left(\delta, p = \gamma + j\frac{n\pi}{\beta}\right) (-1)^n \right] \quad (15)$$

which is the inversed Laplace transform of  $\bar{\Theta}(\delta, p)$ . For faster convergence, numerical experiments have shown that a value satisfying the relation  $\gamma\beta = 4.7$  gives satisfactory results in most cases [13].

### B. Pulsed Laser Heating Source

Assuming that the distribution of the pulsed laser energy is a function of radius with a Gaussian profile, the pulsed volumetric heating is expressed as

$$S(r, t) = 0.94Jg \left( \frac{1-R}{t_p} \right) e^{-g|a-r| - (b|t-2t_p|/t_p)}. \quad (16)$$

Employing the same scheme for the nondimension variable, the Laplace transform, and boundary conditions, one gets the differential equation with respect to the nondimensionless variables in the Laplacian transform domain, which takes the same form as (14), but with the following coefficients:

$$A_i = \frac{(1 + \tau_{qri}p)p}{\alpha_{ri}(1 + \tau_{Tri}p)} \quad D_i = \frac{(1 + \tau_{qri}p)\bar{W} - \tau_{qri}W(\delta, 0)}{K_{ri}(1 + \tau_{Tri}p)}$$

where  $\bar{W}(\delta; p) = W_0\beta_0 e^{-g_0\delta} [(e^{-2b} - e^{-2p\beta_p}/p\beta_p - b) + (e^{-2p\beta_p}/p\beta_p + b)]$ ,  $W(\delta, 0) = W_0 e^{-g_0\delta - 2b}$ ,  $W_0 = 0.94Jg(1 - R/t_p)/(k_r T_r/\alpha_r \tau_{qr})$ ,  $g_0 = g\sqrt{\alpha_r \tau_{qr}}$ ,  $\beta_p = t_p/\tau_{qr}$ , and if  $i = 2$ ,  $D_2 = 0$ .

### C. Steady-State Solution

For the purpose of comparison between the transient temperature and the steady-state temperature, the solution of the

steady-state nondimension temperature is also presented without detail derivation as

$$\Theta_1 = -\frac{W}{6K_{r1}}\delta^2 + \frac{2a^2k_1W + a^2k_2W}{6k_2\alpha_1\tau_{q1}} \quad (17)$$

$$\Theta_2 = \frac{k_1a^3W}{3k_2\alpha_1\tau_{q1}\sqrt{\alpha_1\tau_{q1}}}\frac{1}{\delta}.$$

### IV. PHASE LAG PARAMETERS $\tau_T$ AND $\tau_q$

Since both microstructured effect and microtemporal effect have been lumped into the resultant delayed response in time, the constant value of  $\tau_T$  and  $\tau_q$  are crucial for the description of the heat transport in microscopic scale. However, the determination of  $\tau_T$  and  $\tau_q$ , either theoretically or experimentally, remains a problem. For metal film with regular arrangement of crystal, by comparing DPL model with the hyperbolic two-step model [22], Tzou [13] developed the direct relationship of the two characteristic time constants with the microscopic thermal properties, which is

$$\alpha = \frac{K}{C_e + C_l}, \quad \tau_T = \frac{C_l}{G}, \quad \text{and} \quad \tau_q = \frac{1}{G} \left[ \frac{1}{C_e} + \frac{1}{C_l} \right]^{-1} \quad (18)$$

where  $G$  is a function of electron mass, electron gas density per unit volume, Planck constant, Boltzmann constant, and Debye temperature. By using (18), Tzou obtained  $\tau_q = 0.744$  ps and  $\tau_T = 89.28$  ps for gold film. These two parameters picture the electron–electron and electron–phonon relaxation process.

As the particle temperature increases, energy transfer process from particle to its surrounding medium begins to take place through phonon–phonon coupling. This process determines how long the particle remains being heated without heat dissipation toward surrounding medium. Unfortunately, the thermal relaxation time of biotissue is still in dispute. No unified conclusion has been reached due to the complexity of tissue components. Vedavaz *et al.* [24] used the expression  $\tau_{\text{phonon}} = 3\alpha/v^2$  to estimate the value of relaxation time of biological tissue, which is 1–100 s at room temperature. Mitra *et al.* [25] performed four experiments with different boundary conditions and found that  $\tau_q$  in the processed meat was about 16 s and  $\tau_T$  was about 0.043 s. Kaminski *et al.* [26] estimated that  $\tau_q$  is in the range of 20–30 s. Banerjee *et al.* [27] used relaxation time of 5 s to carry out the theoretical non-Fourier hyperbolic heat analysis and found that it is closer to the experiment results than that with the parabolic Fourier heat conduction.

It should be noted that although the main component of biotissue is water, the experimental relaxation time of gold nanoparticle to water is far smaller than that presented before. Hu and Hartland [28], and Hartland [29] experimentally concluded that

$$\bar{\Theta}_1(\delta; p) = \frac{D_1}{A_1} \left( 1 + \frac{E_2\lambda_1(1 + \sqrt{A_2}\lambda_1)(e^{(\lambda_1+\delta)\sqrt{A_1}} - e^{(\lambda_1-\delta)\sqrt{A_1}})}{E_1(1 - e^{2\sqrt{A_1}\lambda_1} + \sqrt{A_1}\lambda_1(1 + e^{2\sqrt{A_1}\lambda_1})) + E_2(e^{2\sqrt{A_1}\lambda_1} - 1)(1 + \sqrt{A_2}\lambda_1)} \right)$$

$$\bar{\Theta}_2(\delta; p) = \frac{D_1}{A_1} \frac{1}{\delta} \frac{E_1\lambda_1(1 - e^{2\sqrt{A_1}\lambda_1} + \sqrt{A_1}\lambda_1(1 + e^{2\sqrt{A_1}\lambda_1}))e^{(\lambda_1-\delta)\sqrt{A_1}}}{E_1(1 - e^{2\sqrt{A_1}\lambda_1} + \sqrt{A_1}\lambda_1(1 + e^{2\sqrt{A_1}\lambda_1})) + E_2(e^{2\sqrt{A_1}\lambda_1} - 1)(1 + \sqrt{A_2}\lambda_1)} \quad (14)$$

TABLE I  
THERMAL PARAMETERS

	$k$	$\tau_T$	$\tau_q$	$\alpha$
Gold	315	89.28 ps	0.744 ps	$1.18 \times 10^{-4}$
Tissue	0.80	0.043 s	16s	$1.40 \times 10^{-7}$

the time scale of energy dissipation from gold nanoparticle to environments depended on both particle size and surrounding medium. An approximation relationship  $\tau = 0.64R^2$  ps was suggested for gold nanoparticle in aqueous solution by Hu and Hartland, where  $R$  is particle radius in nanometers. In this way, heat is transferred around 580 ps from gold nanoparticles with radius 30 nm into the nearby water shell. However, it is doubtful whether the relaxation time of water can be comparable to that of tissue. This is because animal tissue is a kind of material with air leak. Its thermal properties may depend greatly on the volume fraction of air gap. The thermal insulation effects of air gap have already proved by Lapotko, who reported that vapor bubble generated around nanoparticle is irradiated by pulsed laser with larger fluence. The bubbles, in turn, prevent the heat inside the nanoparticle from being transferred into environments, and then, the temperature of gold nanoparticle may dramatically increase to the melting point, without causing temperature of surrounding medium too high [30], [31]. Ekici *et al.* interpreted the heat transfer from nanorods to surrounding water in another way [32]. A two-temperature model was first used for gold nanorods, and then, an equivalent thermal interface conductance was employed to describe the outgoing heat transfer. The results show gold nanoparticle was close to melting point under certain fluence.

The aforementioned facts indicate that the heat transfer process from nanoparticle to surrounding water is greatly changed by the vapor bubbles. This, to a certain degree, implies that the tissue with air gap may significantly differ from water, as far as the thermal relaxation time is concerned. The exact parameter differences between water and tissue obviously need further investigation. In this study, however, we put an emphasis on the analysis of the overheat phenomenon caused by the larger relaxation time of surrounding medium compared to gold nanoparticle with less focus on what the exact characteristic time of the tissue will be.

## V. RESULTS AND DISCUSSIONS

### A. Temperature Response With Constant Heat Source

We first consider a solid spherical gold particle with radius of 30 nm embedded in infinite tissue-like medium. Constant heat is applied inside the particle at  $t = 0$ . The initial temperature and the temperature at infinite distance are assumed to be  $T_0$ , with thermal physical properties assumed constant. The lag phase of temperature gradient and heat flux vector  $\tau_T$  and  $\tau_q$  are finally given in Table I [13], [23], [24].

In order to verify the analytical solution, we first set  $\tau_T = \tau_q = 0$  in the program, thus the DPL model reduces to a diffusion

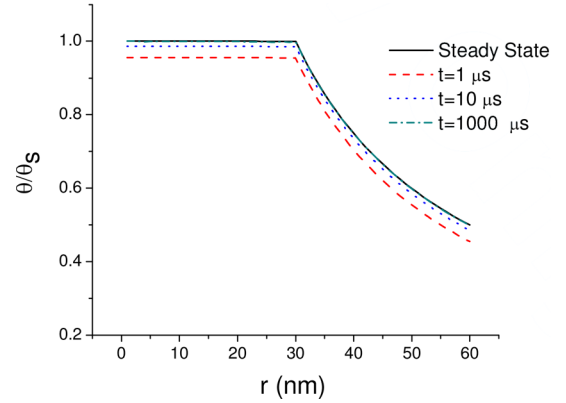


Fig. 2. Dimensionless temperature distribution of diffusion model.  $\theta_s$  is the maximal steady-state temperature of the particle.

model. The temperature distribution was compared with that of the steady-state case (see Fig. 2).

The results show that all the temperature curves take the same form and the transient temperature converges to the steady state with time increasing. Transient process seems to finish within about 10  $\mu$ s. Inspection of the results further indicates that the temperature inside the particle is almost uniform. This is expected as gold has a much higher thermal conductivity than the tissue. For this reason, hereafter in Figs. 3 and 4, only one point on the interface ( $r = 30$  nm) was calculated to represent the temperature of the whole particle. On this basis, the DPL model with different values of  $\tau_{q2}$  and  $\tau_{T2}$  was calculated to explore how these phase lag parameters affect the temperature response in very short time scale. In Fig. 3,  $\tau_{q1}$  and  $\tau_{T1}$  are assigned the actual value of gold. The variable  $\tau_{q2}$  holds constant, while  $\tau_{T2}$  varies. The ratio of  $\tau_{q2}/\tau_{T2}$  were assigned from 0.01 to 5.

Evidently, when  $\tau_{T2} \leq \tau_{q2}$ , a sharp wavefront was observed in the temperature history, as shown in Fig. 3(a) where the temperature evolution at the nanoparticle–tissue interface is displayed. When  $\tau_{T2} = 0$  ( $B = 0$ ), the DPL model reduces to the CV wave equation, and the transient maximal temperature is almost 13 times as that predicted by the diffusion model ( $B = 1$ ). The overshooting phenomenon is caused by the significant phase lag of heat flux of the outer material. As is well known, in a DPL model, the microstructural effect and microtime effect are lumped into two delayed response times to represent the microscopic heat conduction in a material. The DPL model is therefore a macroscopic description of the microscopic effect in both spatial and temporal scales. In the case of  $\tau_{T2} \leq \tau_{q2}$ ,  $\tau_{T2}$  is the cause, and the temperature gradient drives the heat flow. However, the heat flow from interface to the outer tissue material does not follow the temperature gradient simultaneously. In fact, it lags behind the temperature gradient. Compared with gold, the surrounding tissue needs a longer time to reach thermal equilibrium. The  $\tau_q$  values of gold and tissue differ greatly, with the former in the order of picoseconds, while the latter in the order of microseconds. This implies that before sufficient collision of phonons in the outer tissue material occurs to allow heat flow to propagate, heat flux in the gold particle will have difficulty transferring outward, thereby resulting in excessive heat

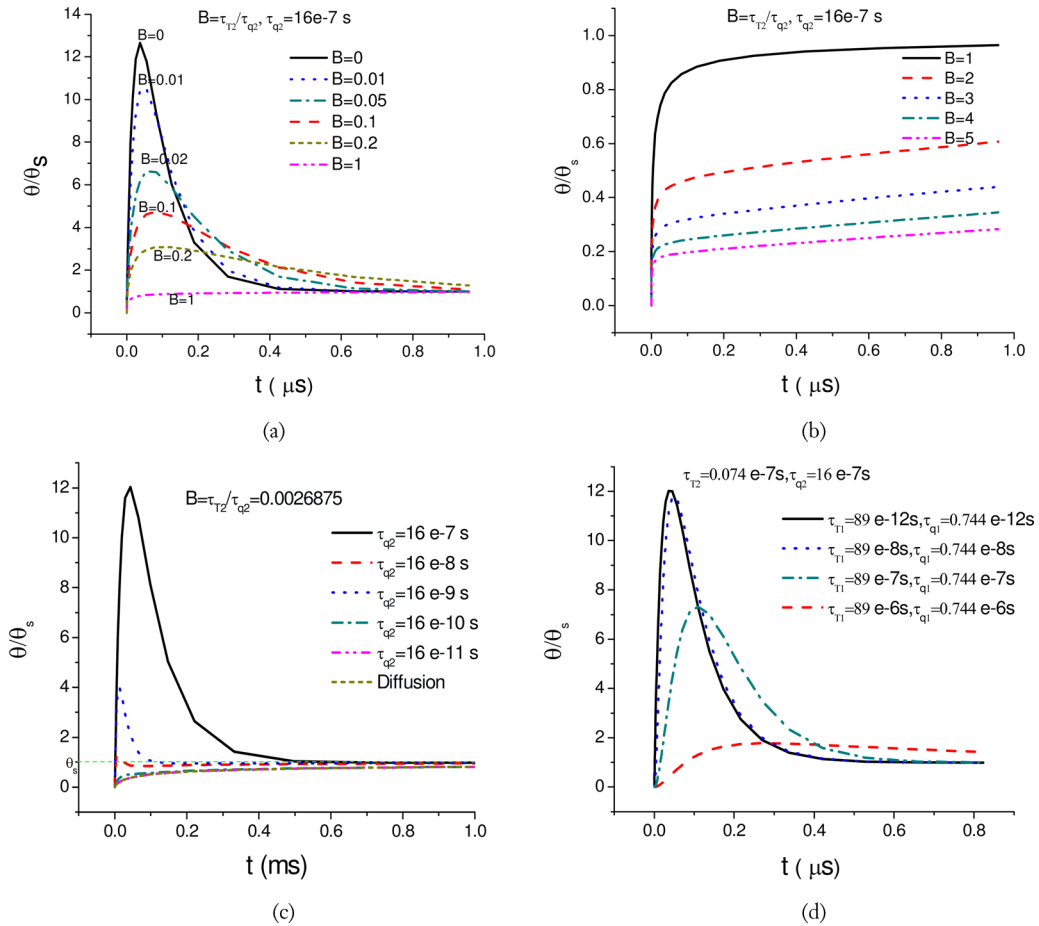


Fig. 3. Effect of characteristic time on transient temperature response. (a)  $\tau_{T2} \leq \tau_{q2}$ . (b)  $\tau_{T2} \geq \tau_{q2}$ . (c)  $\tau_{T2}/\tau_{q2} = \text{const.}$  and  $\tau_{q2}$  varies. (d)  $\tau_{T2}/\tau_{q2} = \text{const.}$ ,  $\tau_{T1}/\tau_{q1} = \text{const.}$ , and  $\tau_{q1}$  varies.

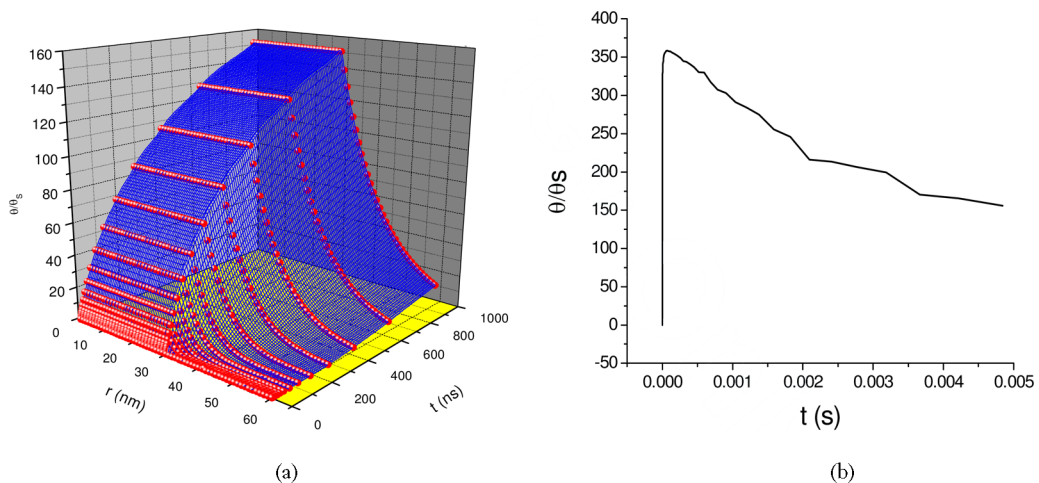


Fig. 4. Temperature distribution, with  $\tau_{T2} = 0.043$  s,  $\tau_{q2} = 16$  s. (a) Temperature versus position and time. (b) Temperature history on the interface of two media.

accumulating inside the particle. Moreover, since  $\tau_{T2}$  is not zero, the equivalent relaxation time becomes  $\tau_2 = \tau_{q2} - \tau_{T2}$ . Obviously,  $\tau_2$  decreases with  $\tau_{T2}$  increasing, when  $\tau_{q2}$  is kept unchanged, which gives rise to a smaller value of  $B$ . A decrease in  $B$  leads to a gradually faster response of the outer material to the

transfer of the heat inside the particle. Physically, this decrease represents the increase of the number of the normal phonon-collision processes (or momentum-conserving collision) versus the number of the umklapp processes (or nonmomentum-conserving collision), the latter being responsible for the heat

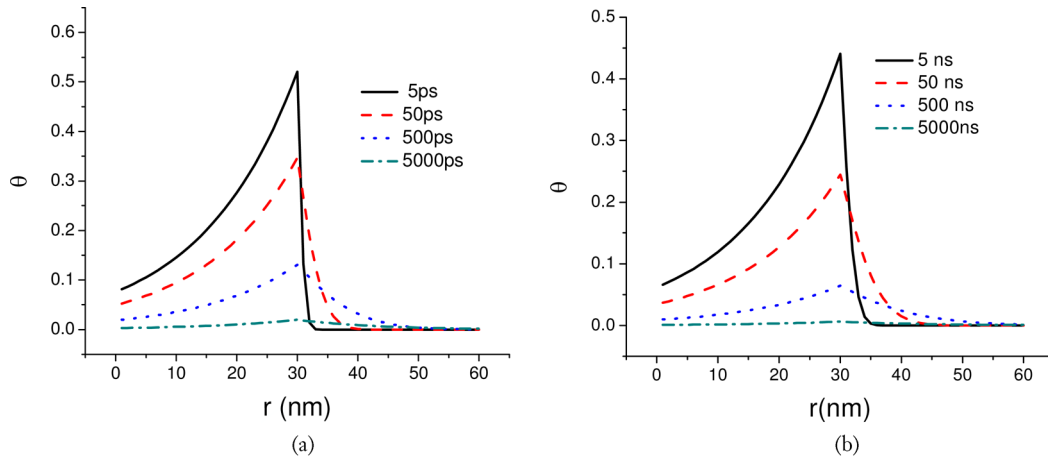


Fig. 5. Dimensionless temperature distribution at different time instant. (a) Diffusion model. (b) DPL model with the actual lagging parameters, i.e.,  $\tau_{T1} = 89$  ps,  $\tau_{q1} = 0.744$  ps,  $\tau_{T2} = 0.043$  s, and  $\tau_{q2} = 16$  s.

flow. If  $\tau_{T2} = \tau_{q2}$ ,  $\tau_2$  becomes zero, then the phase lag phenomenon disappears, implying an instantaneous response from the outer material. The case of  $\tau_{T2} = \tau_{q2}$  gives the same result as the classical thermal diffusion.

Fig. 3(b) illustrates another situation of the microscale effect, where temperature gradient lags behind the heat flux vector. The equivalent relaxation time is negative, which represents the case of overdiffusion. In this case, heat flux is the cause, driving the heat flow. Usually, this phenomenon occurs in metal films. For most dielectric materials, temperature gradient often precedes the heat flux vector. It can be seen that, a bigger  $\tau_{T2}$  produce a higher rate of thermal diffusion. However, a longer time is required to reach thermal equilibrium than that predicted by the classical thermal diffusion model.

Fig. 3(c) shows the case where the ratio of  $\tau_{T2}/\tau_{q2}$  is kept constant, while  $\tau_{T2}$  and  $\tau_{q2}$  are of different order ranging from  $-7$  to  $-11$ . It is apparent that the larger the phase lag, the higher the temperature. It should be emphasized that the temperature is not directly correlated with the ratio. It is the difference of  $\tau_{q2} - \tau_{T2}$  that affects the transient temperature response.

In Fig. 3(d),  $\tau_{T2}/\tau_{q2}$  is kept the same as that in Fig. 2(c), but  $\tau_{q2} = 16e - 7$  s. The characteristic time of metal particle is allowed to vary with  $\tau_{T1}/\tau_{q1}$  held constant. It can be seen that the overshooting phenomenon is diminished by the increase of  $\tau_{T2}$  and  $\tau_{q2}$ . Since in this case,  $\tau_{q2}$  is much larger than  $\tau_{T2}$ ,  $\tau_{q2}$  dominates the transient thermal process. With an increase in  $\tau_{T1}$  and  $\tau_{q1}$ , the difference  $\tau_{q2} - \tau_{q1}$  is decreased. This produces a net result of shortening the response time  $\tau_{q2}$ . As a result, the heat inside the particle is quickly delivered to the surrounding medium without accumulating for long time, thereby relieving the overheating phenomenon.

The aforementioned analysis shows that the fast transient heat transfer process dramatically depends on the characteristic times. The characteristic time of metal is determined to be in the order of picoseconds. However, the accuracy of the parameters for nonlattice structural materials is still in dispute. Nonetheless, the characteristic time of tissue-like material is much larger than that of metal. In addition, the temperature gradient of tissue-like

material precedes the heat flux. These properties result in the fast transient temperature inside the particle and slower response in the tissue, which cannot be predicted by a classical diffusion model.

Fig. 4(a) shows the normalized dimensionless temperature distribution versus position and time. It is seen that with time elapses, temperature inside the particle increases. In addition, the tissue responses are slower compared to diffusion model, presented in Fig. 1. At  $t = 1 \mu\text{s}$ , the ratio of  $\theta/\theta_s$  is about 150. Fig. 4(b) shows the time development of the temperature at the interface between the particle and the tissue. It appears that with a tissue relaxation time of 16 s, the maximal temperature can reach as high as 350 times the steady-state value. Thus, if the steady-state temperature rises by  $0.1^\circ\text{C}$ , the temperature at one time will reach  $35^\circ\text{C}$  at the interface. Since the temperature field contributed by hundreds of thousands nanoparticles is quite different from a single case, additional study is needed to investigate the implication of this fast transient temperature effect related to the hyperthermia treatment.

### B. Temperature Response With a Pulsed Heating Source

In this case, we still investigate the transient thermal response of a solid spherical gold particle embedded in an infinite tissue-like medium. As before, the difference of a diffusion model and the DPL model will be compared first. With the particle material kept unchanged, as well as the geometry size, initial condition, and boundary condition, the influence of characteristic time of surrounding medium on temperature is then studied. Finally, the effect of time duration of the pulse laser is investigated. The only exception with the previous case is the constant heating source replaced by a pulsed laser heating source with a Gaussian profile. The following parameters were used for the pulsed laser:  $J = 13.4$ ,  $R = 0.93$ ,  $g = 1/15.3$ , and  $b = 1.88$ .

The dimensionless temperature with pulsed heating was calculated by employing the diffusion equation and the DPL equation, respectively, and the results are shown in Fig. 5. Here, both the intensity and time duration ( $t_p = 1$  ps) of laser are

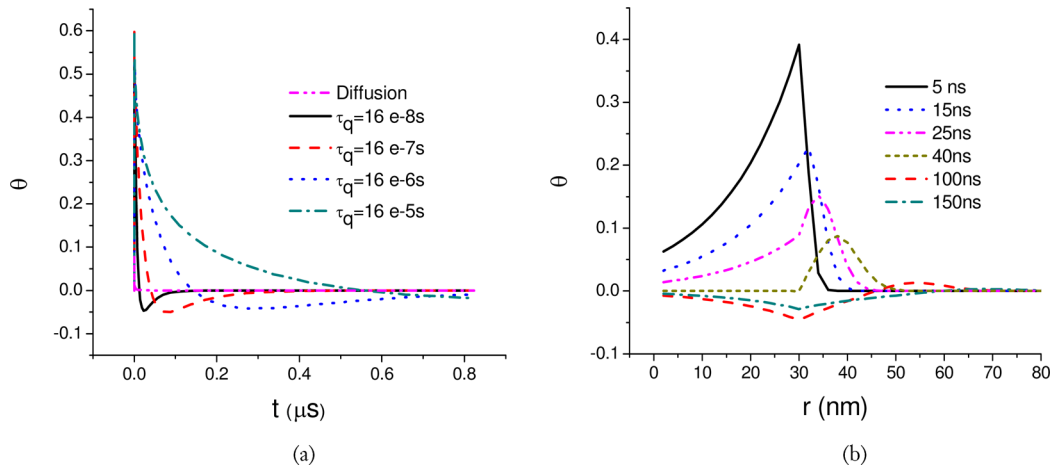


Fig. 6. Effect of  $\tau_{q2}$  on temporal variation of dimensionless temperature,  $r = 30\text{ nm}$ .

same. Fig. 5(a) depicts the dimensionless temperature at four time instants with picoseconds, while Fig. 5(b), with the actual characteristic time, shows the dimensionless temperature with nanoseconds. Apparently, the models produce similar temperature distribution profiles. With time increasing, the dimensionless temperature decreases. This is because the intensity of the pulse laser decays with time. At the beginning, heat diffusion focuses only on the vicinity of the particle. However, with time increasing, heat gradually diffuses outward. This is caused by the damping effect of the small thermal conductivity of tissue.

Besides, comparing curve of  $t = 5000\text{ ps}$  and solid curve of  $t = 5\text{ ns}$  [see Fig. 5(b)], we may find the effect of DPL model on temperature. If we assume that heat flux and temperature gradient take place simultaneously (diffusion model), at  $t = 5\text{ ns}$ , the maximal dimensionless temperature  $\theta_{\text{max}}$  appears in the region of tissue and the value is less than 0.01. However, if we consider the lagging performance (DPL model),  $\theta_{\text{max}}$  is at the interface and the value is about 0.45. The phase lag of heat flux of the tissue  $\tau_{q2}$  dominates the heat conduction process.

With the purpose of understanding the contribution of the characteristic time under pulsed heating, Fig. 6(a) shows the temporal variation of dimensionless temperature at location  $r = 30\text{ nm}$ , i.e., the interface between gold particle and the surrounding media with  $\tau_{T2}/\tau_{q2} = 0.0026875$  and the order of  $\tau_{q2}$  varying from  $-8$  to  $-5\text{ s}$ . All the curves follow the fast-up-slow-down waveform pattern, which corresponds to the profile of the pulsed heating. Also, with  $\tau_{q2}$  decreasing, the diffusion effect becomes evident. In another word,  $\tau_{q2}$  prolongs the diffusion time for heat delivering. It is interesting to note that at some instants, the temperature is lower than the initial value, or the dimensionless temperature is negative. Moreover, the magnitude of the negative temperature depends on the characteristic time, though not linearly. For the values of  $\tau_{q2}$  studied, the dimensionless temperature attains a minimal point at  $\tau_{q2} = 16e-7\text{ s}$ . Further increase in  $\tau_{q2}$  reduces the magnitude of the negative temperature. Fig. 6(b) depicts the transient development of the spatial temperature distribution with  $\tau_{q2} = 16e-7$ , corresponding to the middle curve in Fig. 6(a). It can be seen that

before 40 ns, the dimensionless temperature remains positive, and it gradually evolves into the negative inside and around the particle. The temperature near the interface oscillates both negatively and positively, displaying the nature of thermal wave propagation. Eventually, the oscillation vanishes after sufficient time elapses. As time increases, the thermal wave, generated by a laser pulse, propagates toward infinity, with the magnitude gradually decaying due to the dispersive (diffusive) nature of the materials.

To summarize the factors affecting the temperature distribution, we believe that the negative temperature is an attribute of the wave behavior of the energy transport associated with the hyperbolic description of heat transfer embedded in the DPL model, as well as the geometry shape. In the present case, a heating source whose magnitude decays with both location and time is applied inside the sphere. When heat transfers toward the center of the sphere, the heat transfer area decreases, since it is proportional to the radius squared. Thus, the equivalent heat flux increases when other variables and parameters remained unchanged. When the thermal wave reaches the center of the sphere, reflecting thermal wave appears. The negative dimensionless temperature is a consequence of the incoming and reflecting thermal waves superimposed. At the early stage (e.g., before  $0.1\text{ }\mu\text{s}$ ), more energy is reflected from the particle as time increases, implying that the diffusion mechanism caused by  $\tau_{q2}$  dominates the transient thermal response. Afterwards, the heating source attenuates rapidly with time, but the heat transfer area increases. The combination of these two factors causes the reflective thermal wave to become weaker, and eventually, the thermal diffusivity of the tissue dominates the thermal process. The phenomenon of reflection has also been reported in the literature [16], [17].

## VI. CONCLUSION

Within the framework of the DPL model, the transient heat transfer process of a gold nanoparticle surrounded by tissue was studied for nanoparticle-based hyperthermia applications. Two types of heating sources were considered: one by a constant

heating source, and the other by a pulsed laser. The DPL equations for both the particle and the medium were written in 1-D spherical coordinates and solved using the Laplacian transform. Calculation results show that the temperature predicted by a diffusion equation significantly differs from that by a DPL model. The heat transfer phenomenon in microscopic domains strongly depends on both  $\tau_T$  and  $\tau_q$ . In general,  $\tau_q$  contributes the temperature overshooting, exhibiting the wave behavior, while  $\tau_T$  tends to diminish it, displaying a dispersive nature. The overall thermal behavior is characterized by the lagging phase difference of the nanoparticle and its surrounding medium. For a gold nanoparticle embedded in tissue, a bigger  $\tau_q$  of tissue has a larger effect. It causes heat inside the particle to build locally within a short time. For a constant heating source, the fast transient temperature may be hundred times bigger than that predicted by a classical diffusion equation. Such a high temperature may have a strong implication for hyperthermia treatment and could result in tissue overheating if not controlled. For heating by a pulsed laser, the transient temperature development depends on the time duration of the laser: the shorter the duration, the smaller the transient temperature.

#### ACKNOWLEDGMENT

The authors would like to thank Dr. R. Stevenson for his guidance during the study of this project.

#### REFERENCES

- [1] H. S. Zhou, I. Honma, and H. Komiyama, "Controlled synthesis and quantum size effect in gold coated nanoparticles," *Phys. Rev. B*, vol. 50, pp. 12052–12056, 1994.
- [2] J. B. Jackson, S. L. Westcott, L. R. Hirsch, J. L. West, and N. J. Halas, "Surface enhanced Raman effect via the nanoshell geometry," *Appl. Phys. Lett.*, vol. 82, pp. 257–259, 2003.
- [3] J. L. West and N. J. Halas, "Applications of nanotechnology to biotechnology," *Curr. Opin. Biotechnol.*, vol. 11, pp. 215–217, 2000.
- [4] C. Loo, A. Lin, L. Hirsch, M. H. Lee, J. Barton, N. Halas, J. West, and R. Drezek, "Nanoshell-enabled photonics-based imaging and therapy of cancer," *Technol. Cancer Res. Treat.*, vol. 3, no. 1, pp. 33–40, 2004.
- [5] L. R. Hirsch, R. J. Stafford, J. A. Bankson, S. R. Sershen, B. Rivera, R. E. Price, J. D. Hazle, N. J. Halas, and J. L. West, "Nanoshell-mediated near-infrared thermal therapy of tumors under magnetic resonance guidance," *Proc. Nat. Acad. Sci. USA*, vol. 100, no. 23, pp. 13549–13554, 2003.
- [6] G. G. Akchurin, G. G. Akchurin, and V. A. Bogatyrevb, "Near-infrared laser photothermal therapy and photodynamic inactivation of cells by using gold nanoparticles and dyes," *Proc. SPIE*, vol. 6645, pp. 1U-1–1U-12, 2007.
- [7] T. Q. Qiu and C. L. Tien, "Femtosecond laser heating of multi-layered metals—I. Analysis," *Int. J. Heat Mass Transf.*, vol. 37, pp. 2789–2797, 1994.
- [8] T. Q. Qiu, T. Juhacz, C. Suarez, W. E. Born, and C. L. Tien, "Femtosecond laser heating of experiment multi-layered metals—II. Experiment," *Int. J. Heat Mass Transf.*, vol. 37, pp. 2799–2808, 1994.
- [9] D. Y. Tzou, "On the thermal shock wave induced by a moving heat source," *Trans. ASME J. Heat Transf.*, vol. 111, pp. 237–238, 1989.
- [10] A. Majumdar, "Microscale heat conduction in dielectric thin film," *J. Heat Transf.*, vol. 115, pp. 7–16, 1993.
- [11] Y. Miyamoto, Y. Umebayashi, and T. Nishisaka, "Comparison of phototoxicity mechanism between pulsed and continuous wave irradiation in photodynamic therapy," *J. Photochem. Photobiol. B: Biol.*, vol. 53, pp. 53–59, 1999.
- [12] B. Q. Li, C. Mi, C. H. Liu, G. Cheng, M. Fu, and G. Meadow, "Nanoparticle heat transfer and its application to laser hyperthermia," presented at the ASME Int. Mech. Eng. Congr. Expo. (IMECE 2007), Seattle, WA, Nov. 11–15.

- [13] D. Y. Tzou, *Macro-to-Microscale Heat Transfer: The Lagging Behavior*. Washington, DC: Taylor & Francis, 1996.
- [14] D. Y. Tzou, "Experimental support for the lagging behavior in heat propagation," *J. Thermophys. Heat Transf.*, vol. 9, pp. 686–693, 1995.
- [15] D. W. Tang and N. Araki, "Wavy, wavelike, diffusive thermal response of finite rigid albs to high-speed heating of laser-pulses," *Int. J. Heat Mass Transf.*, vol. 42, pp. 855–860, 1999.
- [16] J. R. Ho, C. P. Kuo, and W. S. Jiaung, "Study of heat transfer in multi-layered structure within the framework of dual-phase-lag heat conduction model using lattice Boltzmann method," *Int. J. Heat Mass Transf.*, vol. 46, pp. 55–69, 2003.
- [17] K. Ramadan, "Semi-analytical solutions for the dual phase lag heat conduction in multilayered media," *Int. J. Thermal. Sci.*, vol. 48, no. 1, pp. 14–25, 2009.
- [18] M. B. Abd-el-Malek and M. M. Helal, "Semi-analytical method for solving nonlinear heat diffusion problems in spherical medium," *J. Comput. Appl. Math.*, vol. 193, pp. 10–21, 2006.
- [19] W. Z. Dai and R. Nassar, "An approximate analytical method for solving 1D dual-phase-lagging heat transport equations," *Int. J. Heat Mass Transf.*, vol. 45, pp. 1585–1593, 2002.
- [20] K. C. Liu, "Numerical analysis of dual-phase-lag heat transfer in a layered cylinder with nonlinear interface boundary conditions," *Comput. Phys. Commun.*, vol. 177, pp. 307–314, 2007.
- [21] R. A. Guyer and J. A. Krumhansl, "Solution of the linearized phonon Boltzmann equation," *Phys. Rev.*, vol. 148, pp. 766–780, 1966.
- [22] T. Q. Qiu and C. L. Tien, "Heat transfer mechanisms during short-pulse laser heating on metals," *J. Heat Transf.*, vol. 115, pp. 835–841, 1993.
- [23] P. J. Antaki, "New interpretation of non-Fourier heat conduction in processed meat," *ASME J. Heat Transf.*, vol. 127, pp. 189–193, 2005.
- [24] A. Vedavarz, S. Kumar, and M. K. Moallemi, "Significance of non-Fourier heat waves in conduction," *J. Heat Transf.*, vol. 116, pp. 221–223, 1994.
- [25] K. Mitra, S. Kumar, A. Vedavarz, and M. K. Moallemi, "Experimental evidence of hyperbolic heat conduction in processed meat," *ASME J. Heat Transf.*, vol. 117, pp. 568–573, 1995.
- [26] W. Kaminski, "Hyperbolic heat conduction equation for materials with a nonhomogeneous inner structure," *ASME J. Heat Transf.*, vol. 112, no. 3, pp. 555–560, 1990.
- [27] A. Banerjee, A. A. Ogale, C. Das, K. Mitra, and C. Subramanian, "Temperature distribution in different materials due to short pulse laser irradiation," *Heat Transf. Eng.*, vol. 26, no. 8, pp. 41–49, 2005.
- [28] M. Hu and G. V. Hartland, "Heat dissipation for Au particles in aqueous solution: Relaxation time versus size," *J. Phys. Chem. B*, vol. 106, pp. 7029–7033, 2002.
- [29] G. V. Hartland, "Measurements of the material properties of metal nanoparticles by time-resolved spectroscopy," *Phys. Chem. Chem. Phys.*, vol. 6, no. 23, pp. 5263–5274, 2004.
- [30] D. Lapotko, "Pulsed photothermal heating of the media during bubble generation around gold nanoparticle," *Int. J. Heat Mass Transf.*, vol. 52, pp. 1540–1543, 2009.
- [31] D. Lapotko, "Optical excitation and detection of vapor bubbles around plasmonic nanoparticles," *Opt. Exp.*, vol. 17, no. 4, pp. 2538–2556, 2009.
- [32] O. Ekici, R. K. Harrison, N. J. Durr, D. S. Eversole, M. Lee, and A. Ben-Yakar, "Thermal analysis of gold nanorods heated with femtosecond laser pulses," *J. Phys. D: Appl. Phys.*, vol. 41, pp. 185501–1–185501-11, 2008.



**Changhong Liu** received the B.S. degree in electrical engineering from Hefei University of Technology, Hefei, China, in 1992, the M.S. degree from Tsinghua University, Beijing, China, in 2001, and the Ph.D. degree from Shanghai Jiao Tong University, Shanghai, China, in 2009.

Since 2001, she has been a Lecturer in Shanghai Jiao Tong University. She is also a Postdoctoral Researcher in the University of Michigan-Dearborn, Dearborn. Her current research interests include electromagnetic field, heat transfer, and cooling

technology.



**Ben Q. Li** received the B.S. degree from the Central University, Hunan, China, in 1982, the M.S. degree from Colorado School of Mines, Golden, CO, in 1984, and the Ph.D. degree from University of California, Berkeley, in 1989, all in mechanical engineering.

He is a Professor and the Chair of the Department of Mechanical Engineering, University of Michigan-Dearborn, Dearborn. For one year, he was a Research Associate with Massachusetts Institute of Technology. He was also a Senior Engineer with Aluminum

Company of America (Alcoa) for three years. He has authored one book and edited two books. He has authored or coauthored more than 200 technical papers in archive journals and conference proceedings. His research work has been supported by various federal (National Science Foundation, National Aeronautics and Space Administration, Department of Energy, Department of Defense, and National Institute for Standards and Technology) and state agencies, as well as private industries. His research interest centers on the study of electromagnetics, fluid flow, and heat transfer in thermal-fluid systems.

Prof. Li has been the invited Keynote Speaker at many domestic and international conferences. He is a Fellow of the American Society for Mechanical Engineers.



**Chunting Chris Mi** (S'00-A'01-M'01-SM'03) received the B.S.E.E. and M.S.E.E. degrees from Northwestern Polytechnical University, Xi'an, China, and the Ph.D. degree from the University of Toronto, Toronto, ON, Canada, all in electrical engineering.

He was with Rare-Earth Permanent Magnet Machine Institute, Northwestern Polytechnical University. In 1994, he joined Xi'an Petroleum Institute as an Associate Professor and an Associate Chair of the Department of Automation. From 1996 to 1997, he was a Visiting Scientist at the University of Toronto. From 2000 to 2001, he was an Electrical Engineer with General Electric Canada, Inc., where he was responsible for designing and developing large electric motors, and generators up to 30 MW. He is currently an Associate Professor and the Director of the DTE Power Electronics and Electrical Drives Laboratory, University of Michigan-Dearborn, Dearborn. He has authored or coauthored more than 80 articles on the subject of electric machines, power electronics, and electric and hybrid vehicles. His current research interests include electric drives, power electronics, electric machines, renewable energy systems, and electrical and hybrid vehicles.

Dr. Mi is currently the Chair of the IEEE Southeast Michigan Section (2008–2009), where he was the Vice Chair from 2006 to 2007. He is the recipient of the National Innovation Award, the Government Special Allowance Award, the Distinguished Teaching Award, and the Distinguished Research Award of University of Michigan-Dearborn. He is also a recipient of the 2007 IEEE Region 4 "Outstanding Engineer Award," the "IEEE Southeastern Michigan Section Outstanding Professional Award," and the "Society of Automotive Engineers Environmental Excellence in Transportation (E2T) Award."